Time and Altitude spread F echoes distribution over the Christmas Island VHF radar

Ricardo Yvan de La Cruz Cueva[1], Eurico Rodrigues de Paula[2], Acácio Cunha Neto[2]

[1]Physics Department, State University of Maranhão, São Luís, Maranhão, Brazil.
5 [2]DIHPA- Heliophysics, Planetary Sciences and Aeronomy Division, National Institute for Space Research, São José dos Campos, São Paulo, Brazil.

Correspondence to: Ricardo Y. C. Cueva (navivacu@gmail.com)

Abstract. The goal of this work is to study the time and altitude echoes characteristics under different solar and seasonality
10 conditions using the VHF radar RTI images. The occurrence of equatorial spread F depends on the existence of conditions that can seed the Raileight-Taylor instability, and these conditions can change with solar flux, seasonality, longitude distributions, and day-to-day variability. So, the equatorial spread F is observed as its time and altitude occurrence. The VHF radar of Christmas Island (2.0º N, 157.4º W, 2.9ºN dip latitude) has been operational in the equatorial region for some time now, allowing long-term observations. The occurrence of echoes during solar minimum conditions are observed all
15 throughout the night, since the post reversal westward electric field is weaker than the solar maximum and the possibilities for the vertical plasma drift to become positive are larger. On other hand, echoes during solar maximum will be controlled by dynamics near the time of the Pre-reversal Peak (PRE). Our results indicate peak time occurrence of echoes along this period shows a well-defined pattern, with echoes being distributed as closer to local sunset during solar maximum and around/closer midnight during solar minimum conditions, meanwhile, the peak altitude occurrence of echoes shows a
20 slightly regular pattern with higher altitude occurrences during solar maxima and lower altitudes during solar minimum conditions.

25

30

1 Introduction

35

The contemporaneous understanding of the formation of F-region plasma irregularities depends mainly on the Rayleigh-Taylor (RT) instability process, due to its appearance at the bottomside of the F-region, then becoming unstable to finally generate plasma bubbles. These recently formed plasma bubbles evolve in nonlinear process then extend into high altitudes

40 into the F-region. The small-scale (centimeter to a few tens of meters) irregularities formed in this process are the responsibles for radar backscatter, which can be observed as structures in the RTI image of the radar. The pioneering ionospheric radar work of Woodman and LaHoz (1976) attributed the term "plumes" to describe radar echoes reaching the topside ionosphere. They observed an slope in the formation of the plumes, then explained using numerical simulation by Ossakow (1981) and Zalesak et al. (1982).

45

The RT instability (and ESF) is controlled by a number of parameters including the prereversal enhancement (PRE) of the zonal equatorial electric field, zonal and meridional neutral winds, longitudinal conductivity gradients, flux tube integrated conductivities, and, possibly, variations in initial (or seed) perturbations (Abdu, 2001; Fejer et al., 1999). It has been noted that ESF bubbles at pre-midnight and post-midnight hours could be driven by different mechanisms (Dao et al., 2011;

50 Yizengaw et al., 2013). The mechanisms that should control the appearance or suppression of equatorial plasma irregularities are different for the pre- and post midnight periods, due to the ambient conditions that prevail along night. Yizengaw et al. (2009) shown that h'F presents a peak at post-midnight hours that indicate the existence of some electrodynamic force that drives the F layer upward creating conditions for irregularities development.

55 The effects of solar and geomagnetic activities on spread-F vary with latitude and longitude. Cueva et al. (2013) examined data from three equatorial stations along solar minimum and maximum conditions. Their results showed that there was an incread in the spread-F occurrence rate with solar flux. Although many researchers have discussed the characteristics of spread-F irregularities at equatorial and low latitudes, some issues are needed of better understanding in their spatial and temporal variability of spread-F and plasma bubbles. So, the analysis of large data were performed in this work covering

60 high and low solar conditions with spread F echoes observations over the Central Pacific region using the VHF radar installed in Christmas Island. In this study we present results from data analysis of echoes distribution using the 50-MHz Christmas Island radar along 2003 and 2012 time period. The observations allowed us to determine how the echoes vary with local time and height throughout different seasons and solar flux conditions.

65

2 Measurements and Analysis

2.1 Data Measurements

70 The Christmas Island VHF radar provides data of meter-scale F-region irregularities routinely, being initially operated by SRI International (2002-2007) and then operated by the US Air Force Research Laboratory (AFRL). The system uses a 100 m x 100 m coaxial collinear (COCO) antenna array. Two stationary beams are used for measurements. One beam is pointed North (azimuth 0º and elevation 84.5º) and the other one is pointed to the east (azimuth 90º and elevation 60.5º). We used measurements made by the North beam only, which is nearly vertical. More technical details of this radar can be found at

75 Miller et al. (2009). Its geographic position is 2.0º N, 157.4º W, 2.9ºN dip latitude, and its magnetic inclination (declination) varied from 4.69º (9.36°E) in 2003 to 4.61º (9.38ºE) in 2012.

It's worth mentioning that measurements available to this study cover different solar conditions when F10.7 varied from 200 SFU (high solar flux conditions) to 66 SFU (low solar flux conditions), as shown in Figure 1. Data measurements of spread

80 F radar echoes to this study are between the period of January 2003 and December 2012. All our data are presented as altitude integration from 200 km to 1000 km height as function of signal to noise ratio (presented in Figure 2), and the horizontal dashed lines (at 20 LT and 00 LT) representing time threshold to assist observation of time-echoes distribution. Lack of data are also presented as black space in the figure, mainly for 2014 (Mach equinox and June solstice).

2.2 Data Analysis

85 Our interest focus in the local occurrence of F-region echoes (5-meter-scale irregularities) as one of the most interesting and challenging phenomenon for space weather and climatological models. The physical mechanism responsible for this phenomenon are complex and not fully understood. So, we had organized our data attempting to present the difference in seasonal and solar flux conditions as a function of time and height of irregularities observed in the VHF-Radar. For this study, we limit our focus to quiet-time irregularities.

90

Is well known that geomagnetic activities directly cause perturbations in the zonal electric field affecting the growth and development of ionospheric irregularities. These influences can be related to the eastward PPEF ("prompt penetration electric field") which behaves increasing the amplitude scintillation in VHF or the westward ionospheric disturbance dynamo electric fields which act suppressing the occurrence of irregularities (Singer et al., 1994; Wang et al., 2008). In

95 sequence, to classify the data with low geomagnetic conditions, we used the 3-hour Planetary K index (Kp). Each measurement was tagged with the value of Kp for the time, of the measurement, plus the previous 3 Kp values. We limited our study to quiet geomagnetic conditions, to be those when none of the three Kp indexes exceeded 3.

Then we sort the seasons for our measurements: Spring Equinox, Summer Solstice, Fall Equinox, and Winter Solstice using
100 91 days of data centered on each day 21 of March, June, September, and December, respectively. We used the quiet time radar echoes, for each season, to obtain the occurrence rate of echoes. We establish that a good representation of irregularity occurrence is given by echoes distribution above 0 dB divided by the total number of observations. Our criterion is a good commitment among being able to identify the occurrence of spread F echoes and to eliminate the effects of non-geophysical echoes.

105

The sample rate of the VHF radar is estimated for every 15-minute intervals starting at 18:00 LT, right before sunset until 05:00 LT near sunrise. To construct maps of irregularity occurrence rate in function of height and local time we had computed for every 15-km height intervals starting at 200 km up to 1000 km altitude.

110 3 Results and Discussions

During solar maximum the spread F events occur near the time when upward drift is large which is promptly after local sunset (Fejer et al., 1999), while during solar minimum when the upward drift is usually short, the spread F exists throughout the whole night, and upward and downward ionospheric conditions may play a role in the morphology of irregularities.
115 Stoneback et al. (2011) showed the role of vertical drift during the extended solar minimum and how it vary from sunset until postmidnight period. These previous work observations increase the need of further study of climatology of echoes evolution in time and altitude.

In the way of understanding this climatology of spread F evolution along seasonality and solar activity we analyzed radar
120 echoes occurrence as function of time and altitude along solar maximum and extended solar minimum period, since the evening vertical drifts and layers heights increase noticeably with solar activity, and along nighttime.

3.1 On the height variability of echo occurrence rates

Peak altitude profiles of the occurrence rate of F-region echoes are shown in Figure 3, top panels. They were organized by seasons (March equinox, June Solstice, September equinox and December solstice, from left to right respectively) along the period of 2003 to 2012. Horizontal dashed lines were placed at 250 and 350 km height to assist observation.

Comparing the peak of altitude echoes along season, we can observe higher occurrence rates of all years over June solstice and September equinox than March equinox and December solstice seasons. This observation match with previous observation by Cueva et al. (2013), that shown the peak occurrence of equatorial spread F for this region being around July-August months. The higher occurrence of echoes in altitude is compared with the density profiles provided by Digisondes.

When observing all years data we conclude that the peak echoes altitude was higher in altitude in June equinox than September solstice, even when its occurrence was the opposite. For the year 2003 and 2012 (high solar flux period) we can mention that peak altitude distribution is the highest, nevertheless present minor percentage of occurrence than solar minimum years (2006 to 2008). The minimum occurrence of peak altitude occurs in March solstice, which is the period of scarce spread F echoes over Christmas Island region.

The altitude distribution of echoes above 350 km also presents same behavior as below this threshold. During solar maximum period radar echoes have less occurrence than solar minimum echoes. During September equinox higher plumes are frequently observed than in other periods, which agrees with results presented by Cueva et al.(2013).

3.2 On the time variability of echo occurrence rates

Time variation in the occurrence rates of F-region echoes for the period in study is shown in Figure 3, lower panels, also separated by seasons (March equinox, June Solstice, September equinox and December solstice, from left to right respectively). The vertical dashed lines represent local sunset and local midnight. As we can observe the percentage of occurrence of echoes presents a solar flux dependence. During solar maximum radar echoes are confined to a few hours after sunset, on the other hand during solar minimum echoes are more broaden out in time and can arise late in the evening after sunset and more closely to midnight hours. As we get closer to solar minimum period the amplitude of echoes occurrence increases due to high probability to occur echoes along all night. This can be observed during years 2006 to 2008 with more amplitude than echoes observed during solar maximum, similar finding was mentioned by Niranjan et al. (2003) when analyzed spread F data from 1997-2000 period, also by Burke et al. (2004) and Dao et al. (2011) using satellite data from different geographical locations.

155

Seasonal dependence of echoes along solar cycle is also observed. September solstice has more conditions to develop irregularities over the region as explained before, as well higher echoes occurrence either for solar minimum and maximum periods. For March equinox and December solstice we have less probability of echoes occurrence as can be seen in the Figure 3, moreover amplitude of echoes occurrence is always lower in solar maximum than in solar minimum.

160

4 Conclusions

The variability over seasonality observed in the amplitude of peak echoes occurrence, either for altitude or time, is suitable for the seasonal spread F occurrence over the Pacific region. Post-midnight events were observed along the solar cycle,

165 decreasing from solar minimum to solar maximum. For the extended solar minimum period, during June solstice and December solstice months, we observed post-midnight echoes similar as previously reported by Otsuka et al. (2012) during 2005 to 2009 period. September equinox also presents post-midnight events for solar minimum period.

These findings are summarized in Figure 4, on top panel is the time peak variation along the period studied separated by

170 seasonality. We can clearly observe the time dependence of echoes with solar cycle, being close to PRE hours in high solar activity and around midnight hours in solar minimum conditions. December solstice during high solar conditions is not following this trend, and further study must be necessary in this point.

Bottom panel on Figure 4 shows altitude peak variation along solar cycle, also separated by seasonality. Altitude parameter

175 seems to follow a very good trend, being higher altitudes for solar maximum conditions and lower altitudes for solar minimum conditions. Again December solstice doesn't match very well with this trend. The altitude parameter is an important parameter due to the key process in the generation mechanism for ionospheric irregularities.

So, for this longitudinal sector we can conclude that during solar maximum conditions we can expect echoes occurring short

180 time after local sunset, and the altitude peak of occurrence around the range of 330 km to 390 km. During solar minimum conditions we can expect echoes around local midnight and around 300 km altitude mainly.

5 Data availability

185 All raw data belong to AFRL Geospace Environment Applications and Impacts Program at Kirtland AFB. Data requirements will be made directly to AFRL directorate.

6 Author contributions

190 Ricardo Y.C. Cueva came up with the idea, prepared all data analysis, then prepared the article draft and final version. E.R. de Paula participated advicing and revieweing the manuscript. Acácio C. Neto gave support with data analysis and equipments.

195 ## 7 Competing interest

The authors declare that they have no conflict of interest.

8 Acknowledgement

200 The authors are very grateful to R.T. Tsunoda and K.M. Groves for providing the VHF radar data from Christmas Island equatorial station, also scknowledgements for the AFRL Geospace Enviroment Applications and Impacts Program at Kirtland AFB. The author E. R. de Paula thank the support from CNPq 202531/2019-0 as well as the INCT GNSS-NavAer grants 2014/465648/2014-2 CNPq and 2017/50115-0 FAPESP.

205

210

9 References

Abdu, M.A: Outstanding problems in the equatorial ionosphere–thermosphere electrodynamics relevant to spread-F, Journal of Atmospheric and Solar Terrestrial Physics 63, 869–884, 2001.

Burke W.J., L.C. Gentile, C.Y. Huang, C.E. Valladares and S.Y. Su: Longitudinal variability of equatorial plasma bubbles observed by DMSP and ROCSAT-1, Journal of Geophysical Research, 109, A12301, doi:10.1029/2004JA010583, 2004.

Cueva R.Y.C., de Paula E.R., and Kherani A.E.: Statistical analysis of radar observed F region irregularities from three longitudinal sectors, Ann. Geophys., 31, 2137-2146, 2013.

Dao E., M.C. Kelley, P. Roddy, J. Retterer, J.O. Ballenthin, O. de La Beaujardiere, and Y.-J. Su: Longitudinal and Seasonal dependence of nighttime equatorial plasma density irregularities during solar minimum detected on the C/NOFS satellite, Geophysical Research Letter, 38, L10104, doi: 10.1029/2011GL047046, 2011.

Fejer B.G., Scherliess L, and de Paula E.R.: Effect of the vertical plasma drift velocity on the generation and evolution of equatorial spread F, J. Geophys. Res., 104, 19859-19869, 1999.

Miller E.S., J.J. Makela, and M.C. Kelley: Seeding of equatorial plasma depletions by polarization electric fields from middle latitudes: Experimental evidence, Geophys. Res. Lett., 36, L18105, 2009.

Niranjan K., P. S. Brahmanandam, P. Ramakrishna Rao, G. Uma, D. S. V. V. D. Prasad, and P. V. S. Rama Rao: Post midnight spread-F occurrence over Waltair ($17.7°$ N, $83.3°$ E) during low and ascending phases of solar activity, Annales Geophysicae, 21: 745–750, 2003.

Ossakow, S. L.: Spread-F theories, J. Atmos. Terr. Phys., 43, 437–452, 1981.

Otsuka, Y., K. Shiokawa, M. Nishioka, and Effendy: VHF radar observations of post-midnight F-region field-aligned irregularities over Indonesia during solar minimum, Indian J. Radio Space Phys. Vol 41, pp 199-207, 2012.

Stoneback R.A., R.A. Heelis, A.G. Burrell, W.R. Coley, B.G. Fejer and E. Pacheco: Observations of quiet time vertical ionos drift in the equatorial ionosphere during the solar minimum period of 2009, Journal of Geophysical Research, 116, A12327, doi:10.1029/2011JA016712, 2011.

Singer, W., Bremer J., P. Hoffmann, A. H. Manson, C.E. Meek, R. Schminder, D. Kürschner, Yu. I Portnyagin, N.A.

250 Makarov, H.G. Muller, E.S. Kazimirovsky, and R.R. Clark: Geomagnetic influences upon tides winds from MLT radars, J. Atmos. Sol. Terr. Phys., 56, 1301 – 1311, doi:10.1016/0021-9169(94)90068-X, 1994.

Tsunoda, R. T.: On the generation and growth of equatorial backscatter plumes: 2. Structuring of the west walls of upwellings, J. Geophys. Res., 88, 4869–4874, 1983.

255

Wang, W., J. Lei, A. G. Burns, M. Wiltberger, A. D. Richmond, S. C. Solomon, T. L. Killeen, E. R. Talaat, and D. N. Anderson: Ionospheric electric field variations during a geomagnetic storm simulated by a coupled magnetosphere ionosphere thermosphere (CMIT) model, Geophys. Res. Lett., 35, L18105, doi:10.1029/2008GL035155, 2008.

260 Woodman, R. F. and La Hoz, C.: Radar observations of F region equatorial irregularities. J. Geophys. Res., 81, 5447–5466, 1976.

Yizengaw E., J. Retterer, E.E. Pacheco, P. Roddy, K. Groves, R. Caton, and P. Baki: Postmidnight bubbles and scintillation in the quiet-time June solstice, Geophysical Research Letter, 40, 1-6, doi: 10.1002/2013GL058307, 2013.

265

Yizengaw E., Maldwin, M.B.; Sahai Y.: and de Jesus R. Strong postmidnight equatorial ionospheric observations during magnetically quiet period, Journal of Geophysical Research, vol. 114, A12308, 2009.

Zalesak, S. T., Ossakow, S. L., and Chaturvedi, P. K.: Nonlinear equatorial spread F – the effect of neutral winds and

270 background Pedersen conductivity. J. Geophys. Res., 87, 151–166, 1982.

275

280

285
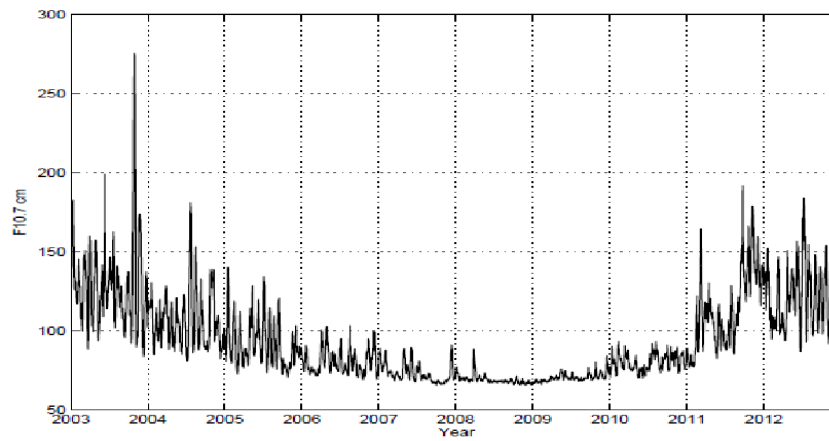
Figure 1: Solar flux index F10.7cm covering period used in this study, which covers solar conditions where F10.7 varied from 200 SFU to 66 SFU.

295

300

305

310
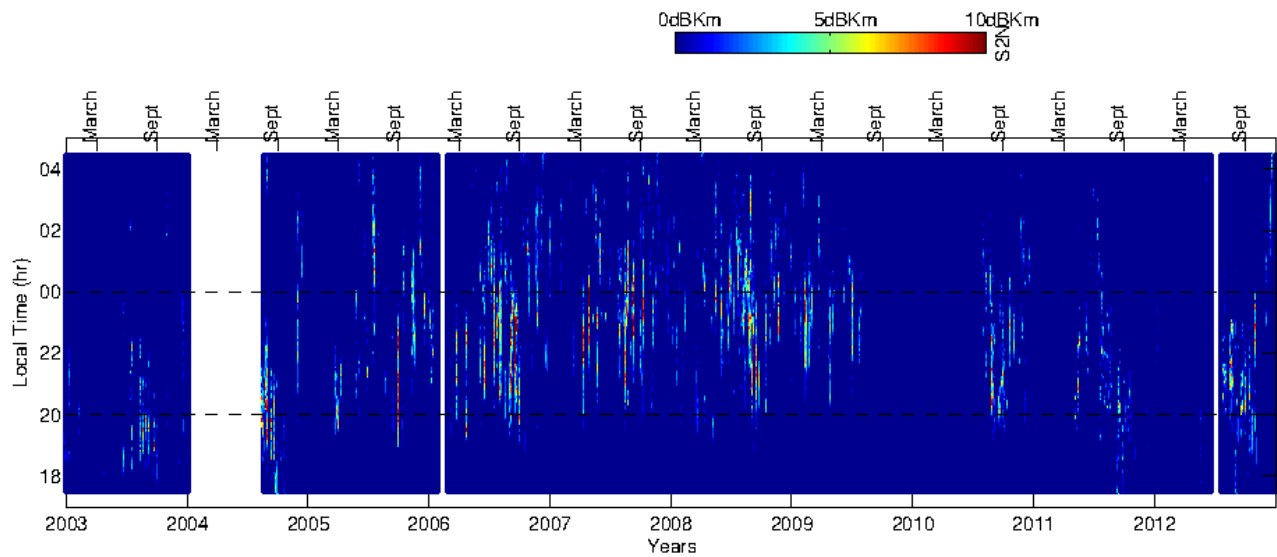
Figure 2: VHF radar data is presented as altitude integration from 200 km to 1000 km height as function of signal to noise ratio
315 **(dBKm), the horizontal lines represent time threshold to help observation of echoes distribution.**

320
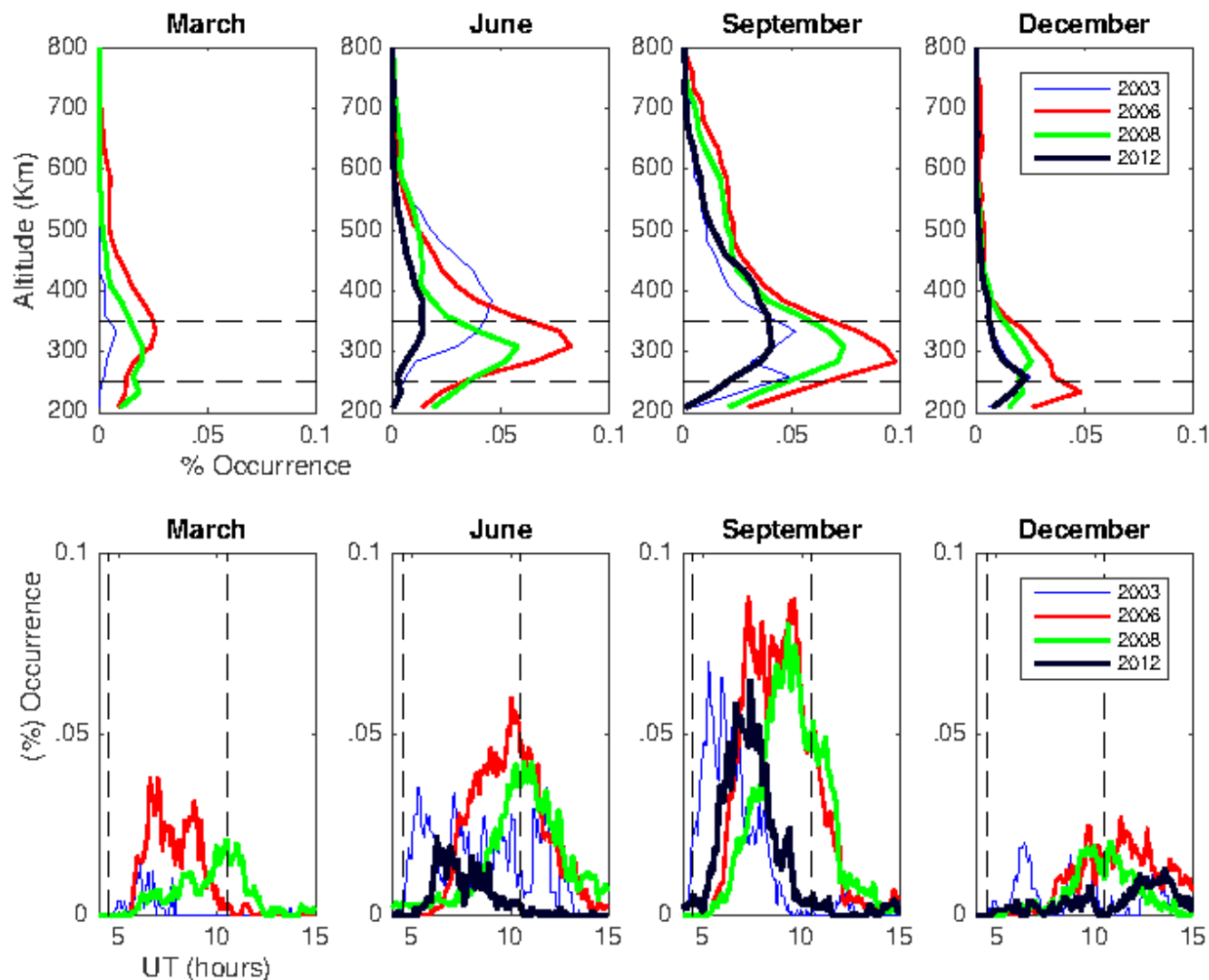
Figure 3: Peak altitude (top panels) and time (bottom panels) variations along the years 2003, 2006, 2008 and 2012 years. Also divided by seasons.

325
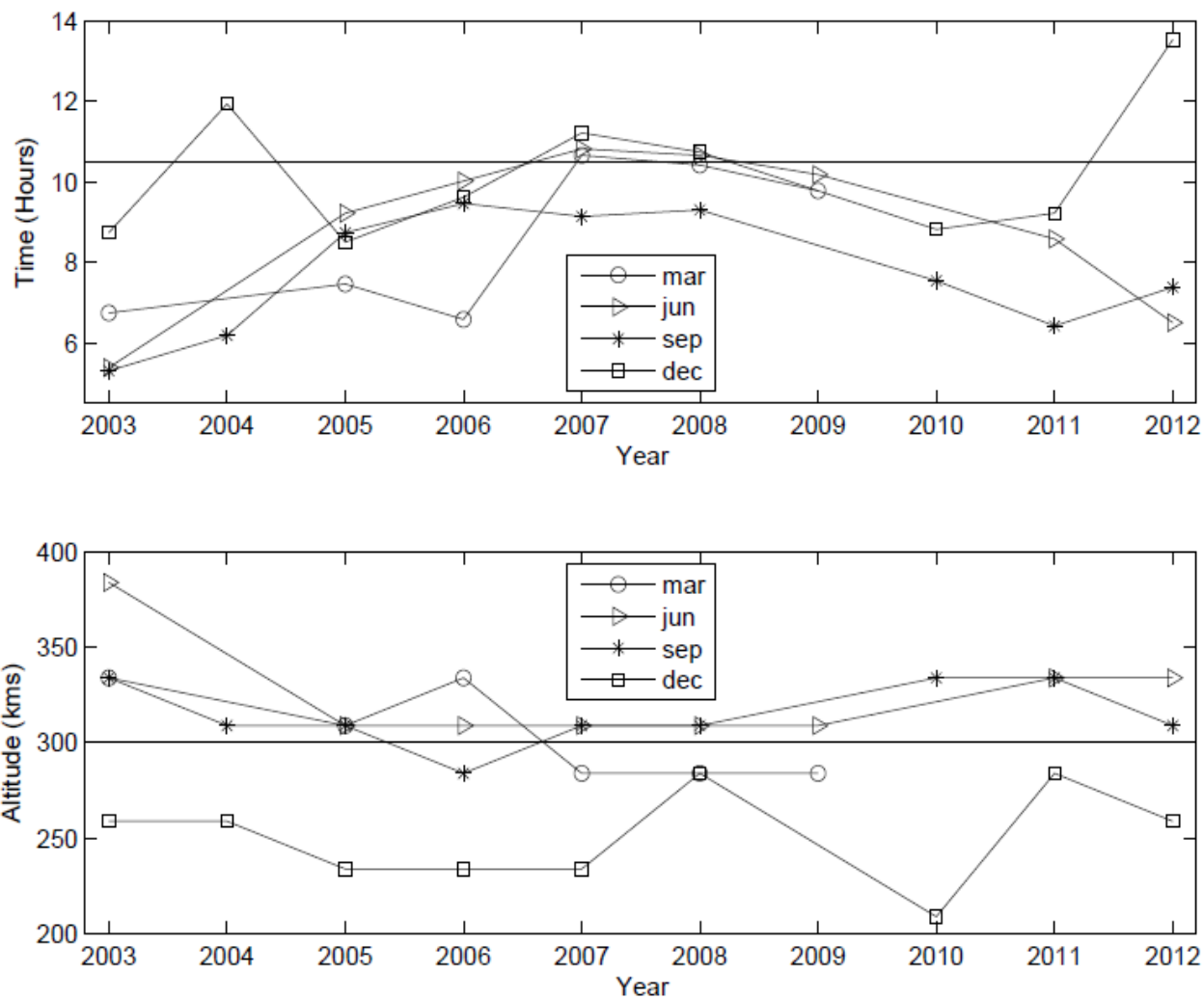
Figure 4: Top Panel: Peak time echoes occurrences along solar cycle and divided by seasons. Bottom panel: Peak altitude echoes occurrences along solar cycle and divided by seasons.